Telemetry in The Classroom: An Excellent Teaching Tool

Michael Rice and David Long
Department of Electrical & Computer Engineering
Brigham Young University
Provo, UT 84602

Abstract

University communications courses typically use broadcast AM and FM as practical examples of fundamental concepts. We propose telemetering based applications which illustrate these fundamental concepts in a more complete manner. This paper presents two simple laboratory experiments which construct simple one-way telemetry links using standard components available in most RF laboratories. The first system is an RS-232 data link and the second system is an analog video system. The performance limitations of these systems illustrate the complexity-performance trade-offs inherent in all communications systems.

Introduction

Communication theory is generally introduced to electrical engineering students in their senior year. Typically, this introduction occurs in a class on analog and digital communications. Such classes provide a brief look at both commercial broadcast and dedicated digital links. The typical teaching approach is lecture which is not always well suited to learning practical concepts of implementation. A preferable method is a hands-on approach. However, it is difficult to provide students with practical, hands-on laboratory experience without spending excessive time on the design and analysis of specific circuits. Wanting to avoid making the class another circuits course, yet desiring to improve the motivation of the students and provide improved insights, we have explored the use of telemetering to illustrate the application of communications concepts in a logical, step-wise fashion.

Our approach is based on some very simple laboratory exercises and the insights gained from trying to improve the performance of the overall telemetry link. We have found that telemetry applications are an excellent introduction to a variety of communications topics. In particular, the concepts of synchronization and link budget follow quite nicely in a telemetry system.

In this paper we describe how a very simple telemetry link based on one-way RS-232 communication over an RF link can be used to introduce and motivate more complicated communications ideas. The analysis of this system leads naturally to the digital communication concepts of bit synchronization, detection, and modulation. A second simple telemetry system to transmit video over a short microwave link is also described. This system is useful for introducing analog communication concepts and tradeoffs including modulation, complexity, and performance. The concept of a link budget arises intuitively from this system. The digital link is described in the Digital Data System section while the analog link is described in Analog Video System section. Discussion, conclusions, and other potential applications for telemetry for communications system education are provided in Results and Concluding Remarks.

Digital Data System

As an example of a digital telemetry link, we consider the establishment of a simple 9600 bit/second wireless RS-232 link. A diagram of the system is shown in Figure 1. The modulation realizes simple binary amplitude shift keying. The RS-232 data stream is converted to a level suitable to driving a mixer connected to a 10 GHz carrier source. The resulting on-off signal is fed to an antenna for wireless transmission of the data. The demodulator is a suboptimal variation of the standard noncoherent detector. The signal available at the antenna terminals is mixed to a quasi-baseband signal by a 10 GHz oscillator which is independent of the oscillator used by the modulator. (The term “quasi-baseband” is used since there is no attempt at carrier frequency or phase synchronization. The signal at the output of the mixer will be offset from "true baseband" by the difference in frequency between the two oscillators and will phaseshifted as well.) The quasi-baseband signal is passed through a Schmitt trigger to create a TTL level NRZ wave form to represent the data. This signal then drives a TTL to RS232 line driver for connection with the serial port of a computer.

Clearly, the design is one which minimized complexity at the expense of performance since no synchronization with the carrier or bit transitions is attempted. The design is not meant to be optimal in any way, but is a design which may be realized using standard components available in most RF laboratories. Such a design leads naturally to a consideration of possible performance improvements realized by improved power amplifiers, coherent demodulators, improved synchronization, etc.

The probability of bit error for this system is derived in Appendix A and is given by

$$P_{snc}(E) \approx \frac{1}{4}\exp\left\{-\frac{A^2}{2N_0B_T}\left(\frac{V_{T-}}{V_{cc}}\right)^2\right\} + \frac{1}{4}\exp\left\{-\frac{A^2}{2N_0B_T}\left(\frac{V_{T+}}{V_{cc}}\right)^2\right\} \quad (1)$$

where

A = the level of the received sinusoid when the carrier is on,

N_0 = the one-sided noise power level,

B_T = the noise bandwidth of the envelope detector,

V_{t-} = the lower threshold point of the Schmitt trigger,

V_{t+} = the upper threshold point of the Schmitt trigger, and

V_{CC} = the power supply voltage of the TTL devices.

The probability of bit error for the ideal non-coherent demodulator using bit synchronization is [1]

$$P_{nc}(E) \approx \frac{1}{2}\exp\left\{-\frac{A^2}{4N_0B_T}\right\} \tag{2}$$

while the probability of bit error for the ideal coherent demodulator using bit, carrier phase, and carrier frequency synchronization is [1]

$$P_c(E) = Q\left(\sqrt{\frac{A^2T}{4N_o}}\right) \tag{3}$$

where Q(•) is the Gaussian tail probability

$$Q(x) = \frac{1}{\sqrt{2\pi}}\int_x^\infty \exp\left\{\frac{t^2}{2}\right\}dt \tag{4}$$

A plot of these three probabilities is illustrated in Figure 3.

For a bit error probability of 10^{-5}, the suboptimal non-coherent system requires a signal to noise ratio of 22 dB while the optimal non-coherent and coherent systems require 13.4 dB and 12.4 dB, respectively. Other modulation formats could also be considered such as binary coherent FSK and binary PSK which require signal to noise ratios of 13.4 dB and 10.4 dB, respectively to achieve a bit error rate of 10^{-5}. This demonstrates several important points:

1. The ideal coherent ASK system requires 10 times less power than the suboptimal non-coherent system. However, the cost is the requirement for carrier frequency and phase recovery together with bit timing synchronization. Thus power and complexity may be exchanged.

2. For a fixed power level, the separation between the transmitter and receiver can be $\sqrt{10} = 3.2$ times greater than that for the suboptimal non-coherent system. Thus distance and complexity may be exchanged.

3. The best performance is realized by the coherent PSK system. It requires 14 times less power or can operate with a transmitter-receiver separation 3.8 times that of the suboptimal noncoherent system. The modulator is more complex, requiring instantaneous 180 degree phase shifts while the demodulator is as complex of any of the other coherent demodulators but is the most sensitive to synchronization errors.

Analog Video System

The analog video transmission system is illustrated in Figure 2 and again uses standard parts available in most RF laboratories. (It was for this reason that balanced double-side-band amplitude modulation was used instead of frequency modulation.)

The experiment consisted of two parts, as shown in Figure 2 to illustrate the importance of carrier phase and frequency synchronization is analog systems. In the first experiment, coherent demodulation as attempted using an oscillator which was independent of the one used for modulation. Expressed mathematically, the video output is

$$\hat{v}(t) = v(t)\cos[\Delta\omega t + \theta] \tag{5}$$

where

v(t) =the video signal,
$\Delta\omega$ = the frequency offset between the receiver oscillator and the carrier, and
Θ =the phase offset between the receiver oscillator and the carrier.

In audio engineering, the frequency offset generates a "warble" effect in the demodulated output. In this case, the frequency offset did not allow sufficient stability to achieve horizontal synchronization on the monitor. The picture quality was, obviously, quite poor.

The second part of this experiment overcame the carrier synchronization problem by using the same oscillator for both the modulator and the receiver. The picture quality was excellent in this case and the effects of carrier frequency offset clearly demonstrated. Connecting the two by cable of course eliminates the need for wireless transmission but does serve to reinforce the necessity of accurate carrier frequency and phase synchronization.

An alternative approach is to use a non-coherent envelope detector together with a transmitted carrier. Given the limited power, poor power efficiency of AM-TC, and low gains of the antennas used, any appreciable transmitter - receiver separation is impossible.

In contrast to the previous experiment, this experiment illustrates the following points:

1. Power and complexity may be exchanged in the system design. This system, however, did not offer sufficient power to allow the simple non-coherent receiver to work.

2. Since the coherent receiver had to be used, the importance of carrier frequency and phase synchronization was illustrated nicely.

Results and Concluding Remarks

Two simple telemetry links constructed with standard parts available in most RF laboratories were described. Neither system was optimal, but served to reinforce the importance of carrier frequency and phase recovery, bit timing synchronization, and complexity-performance trade-offs. The digital system was based on a suboptimal approach to non-coherent ASK. The performance of this system was compared to that of the optimal non-coherent ASK demodulator, the optimal coherent ASK demodulator, and the optimal coherent PSK demodulator. It was shown that increasing the complexity of the demodulator allowed increasing performance (i.e. lower transmit power requirements, or lower bit error rates, or increased transmitter-receiver separation).

The same principles were illustrated with the analog video system. This system however, did not provide sufficient power to allow the use of the simple non-coherent AM envelope detector. Since coherent AM detection was the only option, the effects of carrier frequency and phase offset were clearly demonstrated again reinforcing the importance of the complexity - performance trade-off.

In real telemetering systems, interference and non-ideal components cause performance degradations which can be severe if system selection is not properly done. Typically, a system which is more robust than those presented here is required to realize acceptable performance. Frequency modulation provides more graceful degradation in the presence of interference and component variation which explains the popularity of this approach on test ranges today.

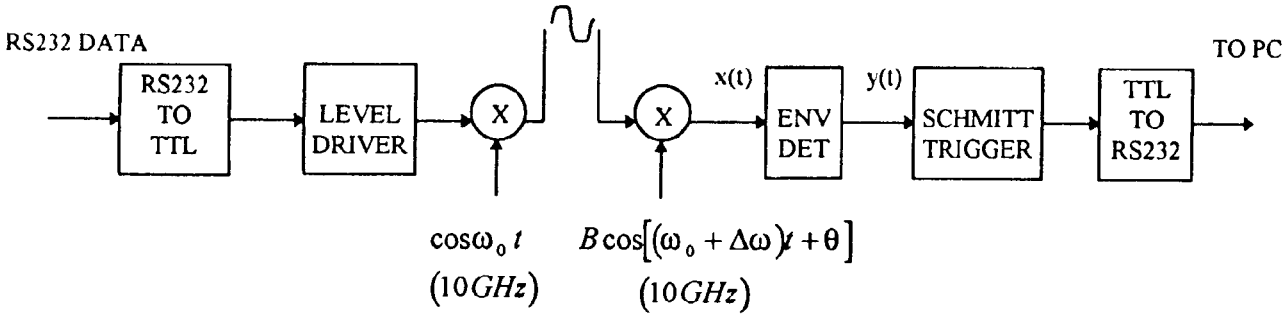

Figure 1: Block Diagram of Sub-Optimal Non-Coherent BASK Data System Using Standard Laboratory Components

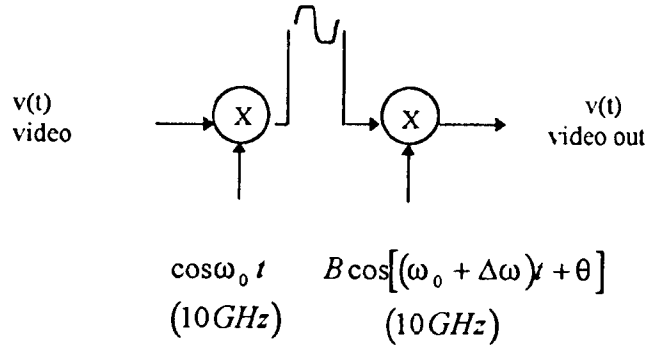

(a) system with no carrier synchronization

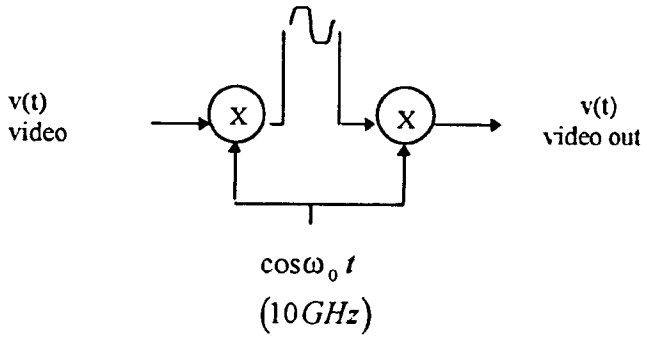

(b) system with fully synchronous carrier

Figure 2: Block Diagrams of Coherent AM Video Systems Using Standard Laboratory Components

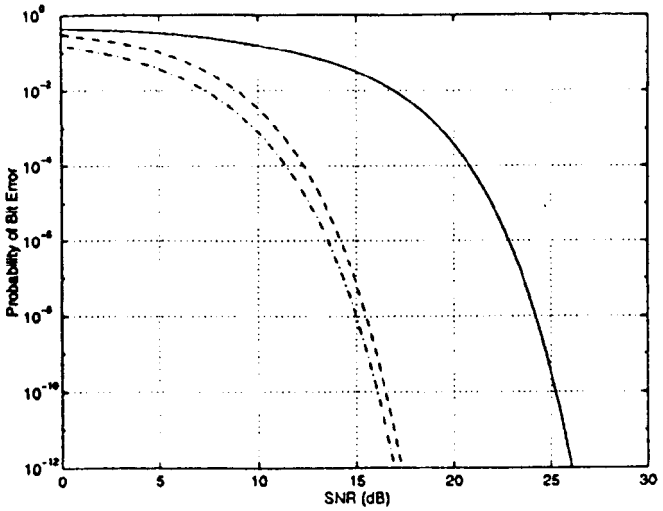

Figure 3: Probability of Bit Error vs. Signal to Noise Ratio for Binary Amplitude Shift Keying. (dash-dot line: Ideal Coherent BASK, dashed line: Optimum Non-Coherent BASK, solid line: Sub Optimum Coherent BASK)

A Performance of The RS-232 Non-coherent ASK System

Let the received signal be

$$r(t) = s(t) + n(t) \tag{6}$$

where

$$s(t)=\begin{cases} 0 \quad 0 \le t \le T \text{ for a } 0 \\ A\cos\omega_0 t \quad 0 \le t \le T \text{ for a } 1 \end{cases} \tag{7}$$

and n(t) is a white Gaussian random process with zero mean and power spectral density $N_0 / 2$.
Suppose a 0 was sent. Then

$$r(t) = n(t) \tag{8}$$

$$= n_c(t)\cos\omega_0 t - n_s(t)\sin\omega_0 t \tag{9}$$

and the mixer output is

$$\begin{aligned} x(t) &= \left[n_c(t)\cos\omega_0 t - n_s(t)\sin\omega_0 t\right] B\cos\left[(\omega_0 + \Delta\omega)t + \theta\right] \\ &\approx \frac{B}{2} n_c(t)\cos(\Delta\omega t + \theta) + \frac{B}{2} n_s(t)\sin(\Delta\omega t + \theta) \\ &= \frac{B}{2}\sqrt{n_c^2(t) + n_s^2(t)}\cos\left[\Delta\omega t + \theta - \tan^{-1}\frac{n_s(t)}{n_c(t)}\right] \end{aligned} \tag{10}$$

The output of the envelope detector is thus

$$y(t)\frac{B}{2}\sqrt{n_c^2(t)+n_s^2(t)} \tag{11}$$

which is described by the Rayleigh probability density function

$$f(y|0)=\frac{y}{N}\exp\left\{-\frac{y^2}{2N}\right\} \tag{12}$$

where

$$N=\frac{B^2 N_0 B_T}{4}. \tag{13}$$

Since the Schmitt trigger uses different trigger levels to transition high to low and low to high, two cases need to be considered when computing the probability of bit error given that a zero was sent:

I . The previously transmitted bit was a zero

2. The previously transmitted bit was a one.

Assuming equally likely 0's and 1's, the probability of bit error given that the transmitted bit was a 0 is

$$\begin{aligned} P(E|0)&=\frac{1}{2}P(E|0,0)+\frac{1}{2}P(E|0,1)\\ &=\frac{1}{2}\Pr\{y>V_{T+}\}+\frac{1}{2}\Pr\{y>V_{T-}\}\\ &=\frac{1}{2}\int_{V_{T+}}^{\infty} f(y|0)dy+\frac{1}{2}\int_{V_{T-}}^{\infty} f(y|0)dy. \end{aligned} \tag{14}$$

Assuming that the gains are set so that BA/2 = V_{cc} the probability of bit error using Equation (12) is

$$P(E|0)=\frac{1}{2}\exp\left\{-\frac{A^2}{2N_0B_T}\left(\frac{V_{T+}}{V_{cc}}\right)^2\right\}+\frac{1}{2}\exp\left\{-\frac{A^2}{2N_0B_T}\left(\frac{V_{T-}}{V_{cc}}\right)^2\right\}. \tag{15}$$

Now suppose a 1 was sent. Then

$$\begin{aligned} r(t)&=A\cos\omega_0 t+n(t)\\ &=[A+n_c(t)]\cos\omega_0 t-n_s(t)\sin\omega_0 t \end{aligned} \tag{16}$$

and mixer output is

$$x(t) = \left[\{A+n_c(t)\}\cos\omega_0 t - n_s(t)\sin\omega_0 t\right] B\cos\left[(\omega_0+\Delta\omega)t+\theta\right] \tag{18}$$

$$\approx \frac{B}{2}\left[A+n_c(t)\right]\cos(\Delta\omega t+\theta)+\frac{B}{2}n_s(t)\sin(\Delta\omega t+\theta) \tag{19}$$

$$= \frac{B}{2}\sqrt{\left[A+n_c(t)\right]^2+n_s^2(t)}\cos\left[\Delta\omega t+\theta-\tan^{-1}\frac{n_s(t)}{A+n_c(t)}\right]. \tag{20}$$

The output of the envelope detector is thus

$$y(t) = \frac{B}{2}\sqrt{\left[A+n_c(t)\right]^2+n_s^2(t)} \tag{21}$$

which is described by the Rice probability density function

$$f(y|1) = \frac{y}{N}\exp\left\{-\frac{y^2+(BA/2)^2}{2N}\right\} I_0\left(\frac{BA}{2N}y\right) \tag{22}$$

where N is given by Equation (13). In this case,

$$\begin{aligned} P(E|1) &= \frac{1}{2}P(E|1,0)+\frac{1}{2}P(E|1,1) \\ &= \frac{1}{2}\Pr\{y<V_{T+}\}+\frac{1}{2}\Pr\{y<V_{T-}\} \\ &= \frac{1}{2}\int_0^{V_{T+}} f(y|1)dy+\frac{1}{2}\int_0^{V_{T-}} f(y|1)dy. \end{aligned} \tag{23}$$

Assuming that the gains are set so that BA/2 = V_{cc} and following the approximations for Equation (22) used in [1], the probability of bit error is

$$\begin{aligned} P(E|1) &\approx \frac{1}{2}\int_{-\infty}^{\frac{BA}{2}\frac{V_{T+}}{V_{cc}}} \frac{1}{\sqrt{2\pi N}}\exp\left\{-\frac{(y-BA/2)^2}{2N}\right\}dy+\frac{1}{2}\int_{-\infty}^{\frac{BA}{2}\frac{V_{T-}}{V_{cc}}} \frac{1}{\sqrt{2\pi N}}\exp\left\{-\frac{(y-BA/2)^2}{2N}\right\}dy \\ &= \frac{1}{2}Q\left(\sqrt{\frac{A^2}{N_0B_T}\left(1-\frac{V_{T+}}{V_{cc}}\right)^2}\right)+\frac{1}{2}Q\left(\sqrt{\frac{A^2}{N_0B_T}\left(1-\frac{V_{T-}}{V_{cc}}\right)^2}\right) \\ &< \frac{1}{2}\exp\left\{-\frac{A^2}{N_0B_T}\left(1-\frac{V_{T+}}{V_{cc}}\right)^2\right\}+\frac{1}{2}\exp\left\{-\frac{A^2}{N_0B_T}\left(1-\frac{V_{T-}}{V_{cc}}\right)^2\right\} \\ &\approx \frac{1}{2}\exp\left\{-\frac{A^2}{N_0B_T}\left(\frac{V_{T+}}{V_{cc}}\right)^2\right\}+\frac{1}{2}\exp\left\{-\frac{A^2}{N_0B_T}\left(\frac{V_{T-}}{V_{cc}}\right)^2\right\}. \end{aligned} \tag{24}$$

The total probability of bit error is obtained by combining Equations (15) and (24) and is given by

$$
\begin{aligned}
P_{snc}(E) &= \frac{1}{2}P(E|0)+\frac{1}{2}P(E|1) \\
&= \frac{1}{4}\exp\left\{-\frac{A^2}{2N_0B_T}\left(\frac{V_{T+}}{V_{cc}}\right)^2\right\}+\frac{1}{4}\exp\left\{-\frac{A^2}{2N_0B_T}\left(\frac{V_{T-}}{V_{cc}}\right)^2\right\} \\
&\quad +\frac{1}{4}\exp\left\{-\frac{A^2}{N_0B_T}\left(\frac{V_{T+}}{V_{cc}}\right)^2\right\}+\frac{1}{4}\exp\left\{-\frac{A^2}{N_0B_T}\left(\frac{V_{T-}}{V_{cc}}\right)^2\right\} \\
&\approx \frac{1}{4}\exp\left\{-\frac{A^2}{2N_0B_T}\left(\frac{V_{T+}}{V_{cc}}\right)^2\right\}+\frac{1}{4}\exp\left\{-\frac{A^2}{2N_0B_T}\left(\frac{V_{T-}}{V_{cc}}\right)^2\right\}.
\end{aligned}
\tag{25}
$$

References

[1] Ziemer, R.E. and W. H. Tranter, Principles of Communications: Systems, Modulation, and Noise, Third Edition, Houghton Mifflin, Boston, 1990.